Rigid-Body Water–Surface Impact Dynamics: Experiment and Semianalytical Approximation

Ravi Challa
Graduate Research Assistant

Solomon C. Yim
Glenn Willis Holcomb Professor

School of Civil and Construction Engineering,
Oregon State University,
Corvallis, OR 97330

V. G. Idichandy

C. P. Vendhan
Professor

Department of Ocean Engineering,
Indian Institute of Technology Madras,
Chennai 600036, India

An experimental study of the dynamics of a generic rigid body during water impact and an equivalent-radius approximate analytical procedure is developed and calibrated in this study. The experimental tests in a wave basin covered a range of drop heights using a 1/6th-scale model of a practical water-landing object prototype for two drop mechanisms to determine the water impact and contact effects. The first mechanism involved a rope and pulley arrangement, while the second mechanism employed an electromagnetic release to drop the rigid body. Hydrodynamic parameters including peak acceleration and touchdown pressure were measured and the maximum impact/contact force was estimated for various entry speeds (corresponding to various drop heights) and weights of the rigid body. Results from the tests show that the impact acceleration and touchdown pressure increases approximately linearly with increasing drop height and the data provides conditions that keep impact accelerations under specified limits for the rigid-body prototype. The experimentally measured maximum accelerations were compared with classical von Karman and Wagner approximate closed-form solutions. In this study, an improved approximate solution procedure using an equivalent radius concept integrating experimental results with the von Karman and Wagner closed-form solutions is proposed and developed in detail. The resulting semianalytical estimates are calibrated against experimental results and found to provide close matching. [DOI: 10.1115/1.4025653]

Introduction

The study of hydrodynamic impact of a moving body on a water free surface finds a variety of applications in the aerospace and ocean engineering fields. The present study is concerned with rigid-body/water–surface impact dynamics of a water-landing object (WLO) in an open ocean using a series of drop tests in a wave basin to assess the maximum force and resulting accelerations. The effect of this impact is prominent in the design phase of the WLO project in determining the maximum design force for material strength determination to ensure structural and equipment integrity and human safety.

Prototype data has been provided by the Indian Space Research Organization (ISRO) to facilitate the making of a physical model of WLO. The prototype used for the Indian space mission is unique in a way that it is conical with a rounded nose (which impacts the water surface first) than compared to the convex shape of the base used for Apollo Command Module (ACM) for the American space missions. This difference precludes meaningful comparison with existing literature available for ACM.

Studies on impact phenomena based on the theoretical and experimental work by von Karman [1] resulted in equations for the impact of rigid bodies on a fluid assuming that the reaction of water was solely due to its inertia. The accelerations and pressures affecting the rigid body were estimated using an approximate expression for the added mass due to the presence of the water. Baker and Westine [2] conducted experimental investigations on a 1/4th scaled model of the Apollo Command Module (ACM) to study the structural response to water impact in both the elastic and failure–initiation regimes. Data from the model tests were compared with results of full-scale experiments. Kaplan [3] examined the specific problem of the ACM impacting water. Their theory and experiments showed that the peak acceleration was proportional to the square of the impact velocity and the results correlated well with the full-scale ACM impact tests. Miloh [4] obtained analytical expressions for the small-time slamming coefficient and wetting factor of a rigid spherical shape in a vertical water entry using experimental data from the ACM tests. A semi-Wagner approach was proposed and then used to compute the wetting factor and the Lagrange equations were employed in order to determine the slamming force from the kinetic energy of the fluid. Good agreement between theoretical model and experimental measurements, both for the early-stage impact force and the free-surface rise at the vicinity of the sphere, was observed. Brooks and Anderson [5] investigated the dynamic response of water-landing space module (WLSM) during impact upon water. A 1/5th-scale model was tested in a three-dimensional (3D) basin at the Oregon State University Wave Research Laboratory and the results were compared with those obtained using analytical techniques and computer simulations. The 3D FE model was validated by comparison with previous full-scale test data and theory. Zhao et al. [6] studied the slamming loads on two-dimensional sections using two different theoretical models. One of the methods is a fully nonlinear numerical simulation that includes flow separation and the other method is an extension of Wagner's solution which does not include the flow separation. Faltinsen [7] studied the theoretical methods for water entry of two-dimensional and axisymmetric bodies. A numerical method was developed and compared against asymptotic methods and validated by experiments for cone and sphere shaped rigid bodies. The significance of the effect of local rise up of the water during entry was identified. Faltinsen [8,9] studied the relative importance of hydroelasticity for an elastic hull with wedge-shaped cross sections penetrating an initially calm water surface. Wagner's theory was generalized to include elastic vibrations. The importance of hydroelasticity for the local slamming-induced maximum stresses increases with decreasing deadrise angle β and increasing impact velocity V. Fair agreement between theory and experiments was documented. Scolan and

Contributed by the Ocean, Offshore, and Arctic Engineering Division of ASME for publication in the Journal of Offshore Mechanics and Arctic Engineering. Manuscript received September 25, 2010; final manuscript received October 5, 2013; published online November 12, 2013. Assoc. Editor: .

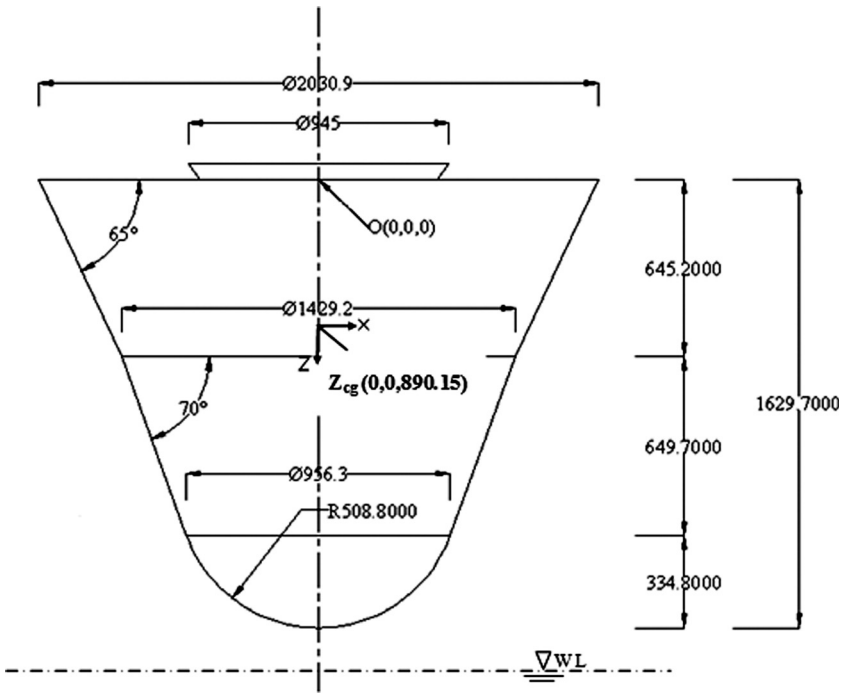

Fig. 1 Overall configuration of WLO prototype (all dimensions are in mm)

Korobkin [10] considered the 3D problem of a blunt-body impact onto the free surface of an ideal incompressible liquid based on Wagner's theory. The three-dimensional nonlinear theory of water impact was solved by Korobkin [11] using the modified Logvinovich model, which is slightly more complex than the Wagner's method used in this study. Scolan and Korobkin [12] performed hydroelastic slamming analysis of a 3D cone using Wagner's approach. The results from their work shows significant influence of the elasticity compared with the rigid case. Seddon and Moatamedi [13] reviewed the work undertaken in the field of water entry between 1929 and 2003, providing a summary of the major theoretical, experimental, and numerical accomplishments in the field.

The physical interpretation of the problem developed by von Karman formed a basis of most of the subsequent works. However, there is little work done on different shaped WLO impacting water surface. The existing experimental data are confined to a convex shaped rigid body impacting water against the much tested concave shaped rigid body (with large base) impacting water surface (US reentry missions). The objective of the WLO drop tests presented below is to study the dynamic response of a conical shaped WLO during water impact by performing drop test experiments using a scaled model with varying heights, measuring their maximum impact acceleration and touchdown pressure. A semianalytical estimation procedure for maximum impact acceleration, based on the von Karman and Wagner closed form solutions and an equivalent-radius approach, is developed and calibrated with experimental results. The predictive capability of the semianalytical estimation procedure is calibrated against experimental maximum acceleration results.

Experimental Investigation of Rigid-Body Impact Dynamics Using Drop Tests

The experimental investigation carried out in the present study on the rigid body (WLO) consists of drop tests from a range of heights. To simulate the dynamic response of the impact experiment for model testing, a 1/6th Froude scale model of the WLO [made of fiber reinforced polymer (FRP)] was used for the experimental drop tests. The overall configuration of the WLO prototype is shown in Fig. 1. Specifications of the prototype and model including the scaling factor for each quantity are shown in Table 1. The WLO was fabricated as a conical shell with a rounded nose. Note that the conical portion (nose part of the rigid body) impacts the water surface. The origin is located at the deck of the WLO and the position of Z_{cg} is measured from the flat base (Fig. 1).

Experimental Test Cases

Two independent sets of drop test are conducted in the experiment. Drop test I involved dropping the rigid body using a rope and pulley arrangement, while drop test II employed an electromagnetic release to drop the model. Both sets of experiments provide valuable and complementary experimental data (for different weight distribution ratios) for numerical model calibration.

The horizontal component of velocity was found to have very little effect on the accelerations in the vertical (Z) direction, in both drop tests the experimental investigations have been confined to vertical drop tests only. Hence, no effort was made to measure either the horizontal component of velocity or was the entry angle varied. (For information on the effect of horizontal speed of the entering body, see Scolan et al. [14].)

Drop Test I

The first set of drop tests was performed recently in the wave basin (30 m × 30 m in plan and 3 m deep) at the Department of Ocean Engineering at IIT-Madras under calm water conditions. Given the maximum clearance of the laboratory, the achievable maximum velocity of impact was estimated to be about 9.81 m/s. This impact velocity was achieved by dropping the model from an overhead crane with a drop height of 5 m above the water surface. The drop tests were carried out over a range at 0.5 m intervals. An important design parameter is the mass, which is selected as 2.03 kg for the test model made of FRP. A skin thickness of 5 mm was selected, with extra thickness at the nose (of about 10 mm) to withstand the force of impact. The estimated values of the center of gravity and moment of inertia are given in Table 1.

The vertical acceleration of the model was measured on impact by using an accelerometer (HMB B12/2000), placed at the center of gravity (CG) of the model. The B12 series Hottinger-Baldwin accelerometers have a frequency response range of 0–1000 Hz,

Table 1 Specification of prototype and model

Property	Full-scale prototype specifications	Scale factors ($\lambda = 1/6$)	Values	Model specifications (1/6th-Froude scale)
Mass of WLO (drop test I)	432 kg	λ^3	0.00462	2.03 kg
Mass of WLO (drop test II)	756 kg	λ^3	0.00462	3.5 kg
Maximum height of the space capsule	1629.7 mm	λ	0.166	271.61 mm
Maximum diameter of the space capsule	2030.9 mm	λ	0.166	338.48 mm
X_{cg}	0	λ	0.166	0
Y_{cg}	0	λ	0.166	0
Z_{cg}	890.15 mm	λ	0.166	147.35 mm
I_{xx}	169.38 kg m^2	λ^5	0.0001286	0.02178 kg m^2
I_{yy}	170.76 kg m^2	λ^5	0.0001286	0.02195 kg m^2
I_{zz}	109.44 kg m^2	λ^5	0.0001286	0.01407 kg m^2

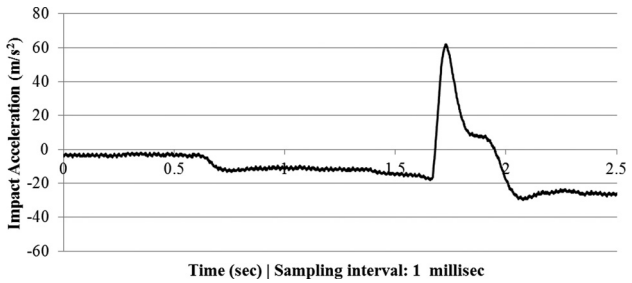

Fig. 2 Measured data of a 5 m drop test: Acceleration time history of a sample test case

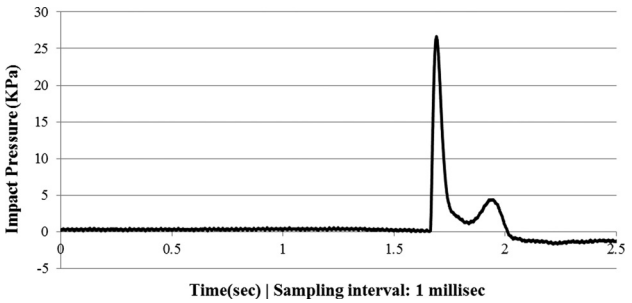

Fig. 3 Measured data of a 5 m drop test: Pressure time history of a sample test case

with an advantage of withstanding impact accelerations up to ±20 g. A 5-bars strain gauge-type pressure transducer (designed and fabricated specifically for the drop tests) is used to calculate the touchdown pressure during impact (mounted at the nose tip with a measuring area of 15 mm ϕ). The motivation behind the use of a diaphragm type strain gauge transducer was the ease of installation, good accuracy, stability, and good shock resistance. The pressure transducer was connected to an MGC amplifier with a full Wheatstones bridge having a sensitivity of 0.1 mV/V.

The accelerometer and the pressure transducer were connected to amplifiers and a PC based data acquisition system was employed to acquire the data. Both the sensors were accurately calibrated and found to be practically perfectly linear with curve-fitted conversion values of less than 0.5% error. [For the accelerometer calibration, 1 V corresponds to 11.1 g and for the pressure sensor, 1 V corresponds to 0.166 bar (0.166×10^5 Pa)].

Impact Test Results—The WLO was dropped, nose down, from various heights to determine the acceleration of the model during the impact and to measure the impact pressure at the nose. Ten seconds of data, with a sampling rate ranging from 1000 to 5000 Hz, were recorded for each drop test to assess the adequacy of sampling rate to capture the peak impact. For the PC based data acquisition, the peak values of acceleration and pressure upon touchdown are found to be consistent after testing for various sampling frequencies. Sample time series for acceleration and pressure for a 5 m drop with a sampling rate of 1 ms are shown in Figs. 2 and 3, respectively. Three identical test runs were conducted for each drop height and the averaged values of the maximum impact acceleration and maximum impact pressures are presented and used in subsequent analysis. The absolute value of the maximum impact acceleration upon impact is approximately 5.2 g and the peak pressure upon impact is 2.6 kPa. The pressure time history depicts that during free fall, the response remains flat ($0 < t < 1.6$ s) and during touchdown on water surface an impulse is recorded ($1.6 < t < 1.8$ s). The post impact pressure scenario clearly shows that the model bounces (with its nose up) after impact ($1.8 < t < 2$ s) and subsequently comes to a static equilibrium with a practically constant submerged pressure ($2 < t < 4$ s).

The details of the pressure distribution during the structural inertia phase are not important as the peak impact pressures are stochastic in nature [15]. Owing to the highly stochastic nature of the peak pressure estimates on the rigid body, each drop test was repeated thrice and the maximum impact pressure reported in Table 2 is the mean value of the three drop test cases.

The variation of peak acceleration and impact pressure values derived using different sampling rates (Fig. 4) demonstrate that the peak values remained consistent (within ±0.8%) for a PC based data acquisition for several trials of drop tests. Figure 5 depicts the consistency of the peak acceleration and pressure (within ±1.0%) for higher sampling frequencies using an oscilloscope capture (0.01 ms to 1.0 μs). The percentage change to show the consistency of the measured acceleration (a) and pressure (p) peaks are calculated by using the formulas $(a_{\text{mean}} - a_{\text{measured}}/a_{\text{measured}} \times 100)$ and $(p_{\text{mean}} - p_{\text{measured}}/p_{\text{measured}} \times 100)$. Since the use of an oscilloscope for measurement during the drop tests was impractical, all further tests used only PC based data acquisition to report the peak accelerations and peak pressures upon impact.

Table 2 gives the values of peak pressure, peak acceleration, and the estimated force acting on the WLO for drop heights ranging from 1 to 5 m with an increment of 0.5 m (comprising of average values of three runs for each drop height). The peak value of acceleration for a 5 m drop height is 52.17 m/s^2 and the peak touchdown pressure is 26 kPa. The total force experienced by the model was obtained using the (dry) model mass multiplied by the measured acceleration (105.9 N for a 5 m drop height). While the theoretical velocity was obtained using the height of drop and a g value of 9.81 m/s^2 (by using the kinematic equation of motion), the experimental velocity was obtained by integrating the measured acceleration time history.

The experimental velocity obtained by integration of the acceleration time history appears to be accurate and in agreement with the observed data. Both theory and experiments showed that the peak acceleration was proportional to the square of the impact velocity. There is a practically linear fit between the force and the square of velocity for various drop heights [3] (Fig. 8).

Table 2 Results for drop test I [weight of WLO = 2.03 kg (drop test I: ordinary drop mechanism)] (vertical entry/entry angle = 0 deg)

Drop height (m)	Acceleration (m/s^2)	Pressure (kPa)	Force (mass × accl.) (N)	Theoretical velocity (m/s)	Experimental velocity (m/s)
5.0	52.17	26	105.90	9.81	9.79
4.5	48.32	23	98.08	9.39	9.27
4.0	45.18	22	91.72	8.85	8.61
3.5	38.76	19	78.69	8.28	8.26
3.0	37.78	18	76.70	7.67	7.55
2.5	33.53	16	68.08	7.00	6.87
2.0	30.27	15	61.45	6.26	6.20
1.5	22.86	13	46.42	5.42	5.31
1.0	11.65	12	23.65	4.42	4.39

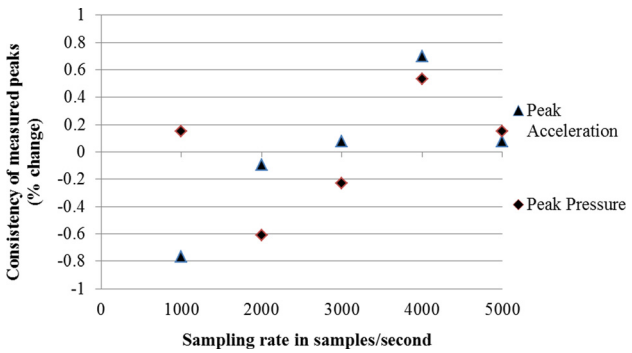

Fig. 4 Consistency of measured peak acceleration and peak pressure versus sampling rate (PC based data acquisition)

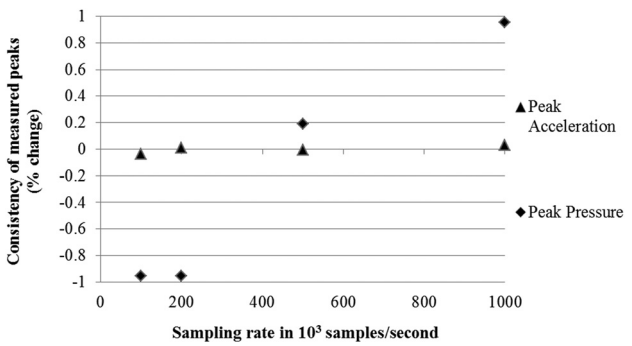

Fig. 5 Consistency of measured peak acceleration and peak pressure versus sampling rate (oscilloscope capture)

Comparison of drop heights to theoretical and experimental velocities showed a very good comparison between both the theoretical and experimental velocities ascertaining the accuracy of the maximum impact accelerations measured experimentally.

Observations also reveal that the touchdown pressures increase practically linearly with the increase in the height of the drop. This linear increase can be attributed to the fact that the experimental results for the maximum impact pressure for each drop height (Table 2) correctly depict what was observed experimentally. The relative importance of hydroelasticity (for small deadrise angles) for an elastic hull with wedge-shaped cross sections [8,9] shows that the impact pressure is practically proportional to the square of the velocity which is well supported by the drop test results (Fig. 9).

Drop Test II

Upon completion of the first set of drop tests presented above, it was decided that a second set of tests with different mass distribution and total weight was warranted. To avoid imprecision in initial condition of the release of the model induced by manual handling (observed during drop test I) and to achieve better control on the point of release, an electromagnetic release mechanism was designed and implemented. A custom designed measuring mechanism on board the WLO enabled the automatic transfer of data in real time to a host computer by means of thin wires. The electronic mechanism along with the steel plate (2 mm thick) was glued to the top of the model, leading to an increase of weight to 3.5 kg. Note that the center of gravity of the WLO for drop test II is different from the first experimental test case.

A steel frame (fabricated in the form of a ladder) was installed on the bridge of the wave basin to hold the electromagnet in position over the water surface. A movable strut was fixed to the steel frame in order to drop the model from every 0.5 m height. The electromagnet was bolted at one end of the strut which would hold the model in position. A switch mechanism, provided on the outer surface of the cap of WLO, activated the data recording just before actuating the release. An up-close view of the setup for drop test II is show in Fig. 6(*a*).

Pressure and acceleration measurements were obtained using built-in amplifiers connected to a computer through a RS485 link. A single axis MEMS-based accelerometer was used to measure the acceleration and a 5-bars strain gauge-type pressure transducer (mounted at the nose tip) measured the touchdown pressure during impact. The accelerometer and the pressure transducer were connected to amplifiers and a PC based data acquisition system was employed to acquire the data in real time. The WLO was dropped using the electromagnetic release from the frame fixed to the bridge. The WLO touchdown with the water surface is shown in Fig. 6(*b*). The model was tested initially for a 0.5 m drop and then the height was gradually increased to 5 m in steps of 0.5 m. The release switch was activated once the model was held to the electromagnet and the acceleration and the pressure data were recorded during the descent. The acceleration and pressure time histories for the single case of a 5 m drop, after analysis in the host computer, are shown in Figs. 7(*a*) and 7(*b*).

Table 3 gives the values of peak pressure, peak acceleration, and the estimated force acting on the WLO for drop heights ranging from 1 to 5 m at an increment of 0.5 m. Note that the peak value of acceleration for a 5.0 m drop height is 36.5 m/s^2 and the touchdown pressure is 41 kPa. The force experienced by the model was obtained using the model mass and measured acceleration (127.7 N for a 5 m drop height). While the theoretical velocity was obtained based on drop height and a g value of 9.81 m/s^2, the experimental velocity in the last column was obtained by integrating the measured acceleration time history. As observed in the first drop test, both the peak acceleration and touchdown pressure increases linearly with the increase in the height of drop. As observed in drop test I, the variation of impact force and the square of the impact velocity, for drop test II, exhibits a practically linear behavior for various drop heights, confirming the results of Kaplan [3] (Fig. 8). The accuracy of the experimental measurements was ascertained by the very good comparison between the theoretical and experimental velocities for various drop heights shown in Table 3.

Fig. 6 Electromagnet with protruding strut: (*a*) Up-close view of the setup for drop test II and (*b*) WLO touchdown with water surface

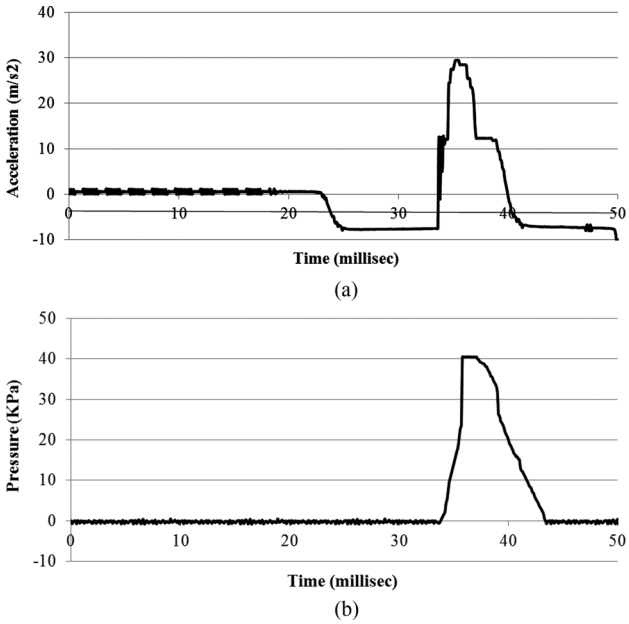

Fig. 7 Measured electromagnetic release data of a 5 m drop test: (*a*) Acceleration time history and (*b*) pressure time history

Note that the maximum force versus the square of the impact velocity (Fig. 8) for drop test I shows deviation from a straight line behavior. This may be attributed to the lack of precise control of the initial point of release of the model, and small sample size (only three) to characterize the stochastic physical nature of the maximum acceleration and impact pressures.

In order to understand the linear variation of maximum impact pressure for each drop height (for both drop tests) a figure showing the variation of the maximum impact pressure and the square of the normalized velocity (normalized using the maximum velocity of impact) are plotted (Fig. 9). The figure depicts a

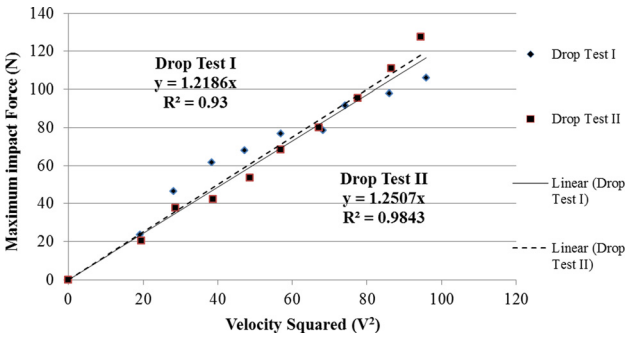

Fig. 8 Maximum impact force versus square of impact velocity (drop tests I and II)

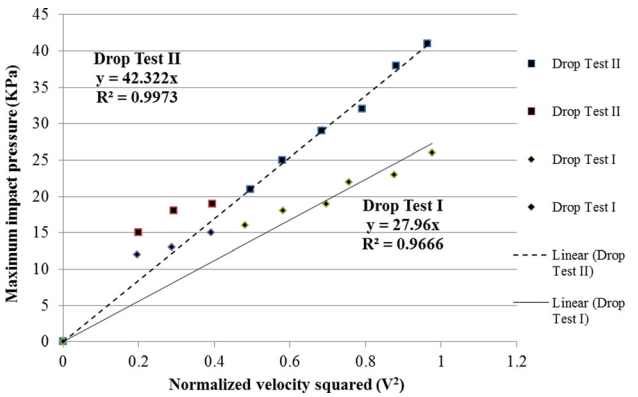

Fig. 9 Maximum impact pressure versus square of normalized impact velocity (drop tests I and II)

Table 3 Results for drop test II [weight of WLO = 3.5 kg (drop test II electromagnetic release)] (vertical entry/entry angle = 0 deg)

Drop height (m)	Acceleration (m/s^2)	Pressure (kPa)	Force (mass × acc) (N)	Theoretical velocity (m/s)	Experimental velocity (m/s)
5.0	36.50	41	127.72	9.81	9.72
4.5	31.72	38	111.02	9.39	9.30
4.0	27.32	32	95.62	8.85	8.81
3.5	22.82	29	79.87	8.28	8.19
3.0	19.55	25	68.42	7.67	7.54
2.5	15.32	21	53.62	7.00	6.97
2.0	12.12	19	42.35	6.26	6.22
1.5	10.72	18	37.52	5.42	5.35
1.0	9.92	15	20.22	4.42	4.42

Table 4 Analytical solution results from von Karman (1929) and Wagner (1932) approaches

WLO drop test cases cone radius: 0.0848 m max. radius: 0.3385 m	Maximum acceleration (experiments) g: acceleration due to gravity (m/S^2)	Analytical solutions for maximum accelerations: von Karman [Eq. (5)] $a_{\max\text{-}\nu K}$	Analytical solutions for maximum accelerations: Wagner [Eq. (10)] $a_{\max\text{-W}}$	Equivalent radius (m) of WLO conical portion: von Karman $r_{\max\text{-}\nu K}$	Equivalent radius (m) of WLO conical portion: Wagner $r_{\max\text{-W}}$
Drop test I: Ordinary drop mechanism	5.2 g	14.7 g	19.8 g	0.0300 m	0.1075 m
Drop test II: Electromagnetic release mechanism	3.6 g	10.4 g	25.2 g	0.0293 m	0.1310 m

"practically" linear relationship which is in accordance with the fact that the pressure is directly proportional to the force acting on the rigid body. However, a closer look at the figure with respect to the actual physics of the impact phenomenon shows that there is a deviation from the linear trendline (first three data points) at low entry velocities (when $v \to 0$). This can be attributed to the fact that the body records a finite impact pressure at low impact velocities resulting in the deviation from the linear trendline shown in Fig. 9.

Approximate Closed Form Solutions for Maximum Impact Accelerations

For a WLO that has a spherical bottom and is assumed rigid, closed form solutions based on the von Karman [1] and Wagner [16] approaches are available for correlating with the results from the experimental analysis [17]. Zhao et al. [6] developed a generalized Wagner model, within which only the boundary conditions on the liquid free surface are simplified (linearized BCs). The von Karman approach is based on conservation of momentum and uses an added mass. The penetration depth is determined without considering water splash-up. The Wagner approach uses a more rigorous fluid dynamic formulation and considers the effect of water splash-up on the impact force. The kinematic free surface condition was used to determine the intersection between the free surface and the body in the outer flow domain. Satisfaction of the kinematic free surface condition implies that the displaced fluid mass by the body is properly accounted for as rise up of the water. This is not true for a von Karman approach that does not account for the local rise up of the water. From the analytical solutions for a spherical bottom body impacting with water using the von Karman method [18], the magnitude of the virtual mass for a spherical bottom body is

$$m_v = \frac{4}{3}\rho h^{3/2}(2R-h)^{3/2} \tag{1}$$

where m_v is the virtual mass, ρ is the mass density of water, h is the penetration depth, and R is the radius of the spherical bottom. The instantaneous velocity V of the center of gravity of the rigid body is

$$V = \frac{dh}{dt} = V_0\left(1+\frac{m_v g}{W}\right)^{-1} \tag{2}$$

where t is time after impact, V_0 is the initial velocity, g is the gravitational constant, and W is the weight of the rigid body. By substituting Eq. (1) into Eq. (2), and assuming $h/r = 1$, the instantaneous velocity can be rewritten as

$$V = \frac{V_0}{1+\dfrac{8\sqrt{2}\rho g R^3}{3W}\left(\dfrac{h}{R}\right)^{3/2}} \tag{3}$$

The overall acceleration a can be written as

$$a = \frac{d^2h}{dt^2} = -\left\{\frac{3\times 2^{1/2}\left(\dfrac{3W}{4\pi\rho g R^3}\right)^2\left(\dfrac{V_0^2}{gR}\right)\left(\dfrac{h}{R}\right)^{1/2}}{\pi\left[\left(\dfrac{3W}{4\pi\rho g R^3}\right)+2^{3/2}\pi^{-1}\left(\dfrac{h}{R}\right)^{3/2}\right]^3}\right\} g \tag{4}$$

Assuming $h/r \ll 1$, the maximum acceleration can be found as

$$a_{\max-\nu K} = -\frac{256}{243}\left(\frac{4\rho g R^3}{3W}\right)^{2/3}\left(\frac{V_0^2}{R}\right) \tag{5}$$

where νK stands for von Karman in (5) and the time at which the maximum acceleration is achieved is given at

$$t_{\max-\nu K} = \frac{21}{160}\left(\frac{3W}{4\rho g R^3}\right)^{2/3}\frac{R}{V_0} \tag{6}$$

and the penetration depth at

$$h_{\max-\nu K} = \frac{1}{8}\left(\frac{3W}{4\rho g R^3}\right)^{2/3} R \tag{7}$$

In the von Karman approach, the rise of water due to the splash-up is not considered. The effect of splash-up was considered by Wagner and found to have significant effect on the impact force. Recently, Miloh [4] used a semi-Wagner approach to determine the nondimensional slamming coefficient that is defined as

$$C_s\left(\frac{h}{R}\right) = \frac{2F}{\rho\pi R^2 V_0^2} \tag{8}$$

where F is the impact force. Based on the analytical derivations, Miloh [4] proposed that

$$C_s\left(\frac{h}{R}\right) = 5.5\left(\frac{h}{R}\right)^{1/2} - 4.19\left(\frac{h}{R}\right) - 4.26\left(\frac{h}{R}\right)^{3/2} \tag{9}$$

is suitable for initial stage slamming. Note the coefficients in Eq. (9) are determined from a set of experimental data from the ACM tests. Based on these analytical derivations the maximum acceleration can be estimated as

$$a_{\max-\mathrm{W}} = \frac{g}{2W}C_s\left(\frac{h_{\max}}{R}\right)\rho\pi R^2 V_0^2 \tag{10}$$

where W stands for Wagner in (10).

Table 4 shows the comparison of the experimental results with analytical solutions. The maximum z accelerations for a vertical entry for both drop mechanisms is compared to the closed form solutions based on von Karman and Wagner approaches.

The equivalent radius is a representative or nominal radius of WLO that yields the accelerations comparable to the maximum

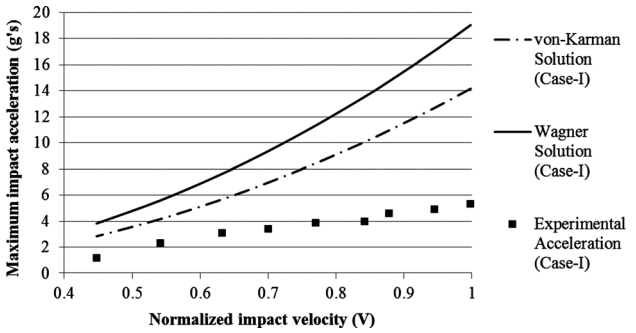

Fig. 10 Maximum acceleration using von Karman and Wagner solutions (drop test I)

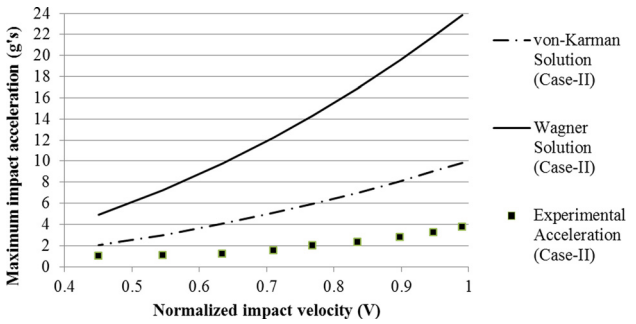

Fig. 11 Maximum acceleration using von Karman and Wagner solutions (drop test II)

impact accelerations obtained experimentally with the conical shaped WLO. From the analytical solutions for a spherical bottom body impacting with water surface, for the von Karman method, Eq. (5) is used to calculate the equivalent radius by computing $r_{\text{max-}vK}$ corresponding the maximum impact acceleration $a_{\text{max-vK}}$ and is given by

$$r_{\max-vK} = R = -\frac{a_{\max-vK}}{V_0^2}\left(\frac{243}{256}\right)\left(\frac{3W}{4\rho g}\right)^{2/3} \tag{11}$$

and correspondingly for the Wagner method, Eq. (10) can be used to calculate the equivalent radius by computing the value of $r_{\text{max-}W}$ corresponding the maximum impact acceleration $a_{\text{max-}W}$ and is given by

$$r_{\max-W} = R = \frac{2Wa_{\max-W}}{\rho g\pi V_0^2 C_s h_{\max}} \tag{12}$$

Values of the "equivalent radius" of the WLO conical portion is also shown in Table 4. A detailed description of the equivalent radius approximate semianalytical procedure is provided in the subsequent section.

It is important to note that the maximum radius of the base (for a 1/6th Froude-scale model of a WLO) is 338.5 mm and the radius of the conical portion impacting the water surface is 84.8 mm. For a WLO model with the dimensions shown in Table 1, the accelerations obtained from both von Karman and Wagner approaches for experimental drop test I are 14.7 g and 19.8 g, respectively (see Table 4). Similarly, the maximum impact accelerations obtained from both the approaches for drop test II are 10.4 g and 25.2 g, respectively. Figures 10 and 11 show the normalized values of maximum impact accelerations plotted and normalized impact velocity for both the experimental cases and the corresponding analytical solutions. (Note that all the *abscissas* in the graphs have been normalized using $\sqrt{2gh}$, which is the maximum velocity upon impact for both the drop tests.)

For a conical bottomed rigid body, the analytical results show that there is a large difference between the experimental peak impact accelerations and those obtained by von Karman and Wagner analytical estimates. The large difference can be attributed to the conical shape of the WLO bottom impacting the water surface compared to the large spherical bottom used in deriving the closed form solutions. It can be deduced from Table 4 that for a conical bottomed rigid body (like the WLO), the experimental values of peak impact accelerations (for a 0-deg pitch), do not fit in the bounds on maximum impact accelerations calculated by both von Karman and Wagner approaches.

In addition to the unique shape of the WLO (which is primarily responsible for the large deviation of the experimental impact accelerations from the closed form solutions) the basic assumptions of the formulations for both von Karman and Wagner approaches also play a pivotal role in contributing to the large difference. Also, the continuously varying deadrise angle for the WLO convex shaped rigid body impacting water significantly influences the maximum impact acceleration of the experimental results compared to the closed form solutions provided by von Karman and Wagner for constant small deadrise angles. The von Karman approach is based on conservation of momentum (using an added mass) and the penetration depth is determined without considering water splash-up; thus neglecting the highly nonlinear coupled fluid–structure interaction effect. The Wagner approach, on the other hand, attempts to relax the von Karman no-splashing assumption by using a rigorous dynamic formulation and incorporates the effect of the upward splashing of the water and its effects on the motion of the rigid body. With the upward splashing correction, the Wagner approach tends to overpredict the maximum impact retardation as it neglects nonlinear effects near the impact zone.

The lack of agreement in the peak acceleration obtained in the present experimental study with the closed form von Karman and Wagner approximate solutions is due to the large initial angle at impact and the relatively rapid changes in contact radius of the inverted cone shape of the WLO as it penetrates the water surface. These deviations from the idealized assumption may be taken into account using the concept of an equivalent radius.

An Equivalent Radius Approximate Semianalytical Procedure. In order to capture the proper modeling of the dynamics of the impact and to ascertain a true fluid behavior, an attempt was made to calculate an equivalent radius of the conical portion of the WLO that would compare well with the experimental maximum impact accelerations [Eqs. (11) and (12)]. Figure 12 shows a representative equivalent radius of a conical shaped WLO model using von Karman/Wagner approaches (with values summarized in the rightmost column of Table 4).

From the von Karman approach the equivalent radius for drop tests I and II are 30 and 29.3 mm, respectively. It can be observed that the von Karman approach tends to estimate a lower value of the radius of the conical portion. As the effect of local rise up of the water is significant during water entry of a rigid 3D rigid body, the von Karman predictions for maximum impact accelerations are not significant in determining the maximum impact accelerations for the water entry of the WLO. The Wagner approach, on the other hand, estimates the equivalent radius for drop test I and drop test II as 107.5and 131 mm, respectively. Based on the equivalent radius approach, approximate semianalytical solutions based on the von Karman and Wagner theories can be used to obtain design maximum accelerations of the WLO model consistent with experimental results. In order to further comprehend the effect of the shape of the rigid body (especially the conical portion of the WLO impacting the water surface first), the values of equivalent radius (r) are plotted against different normalized velocities of impact for both drop test I and II (Fig. 13). The equivalent radius (r) was initially obtained for each drop velocity for both the experimental cases. The idea is to

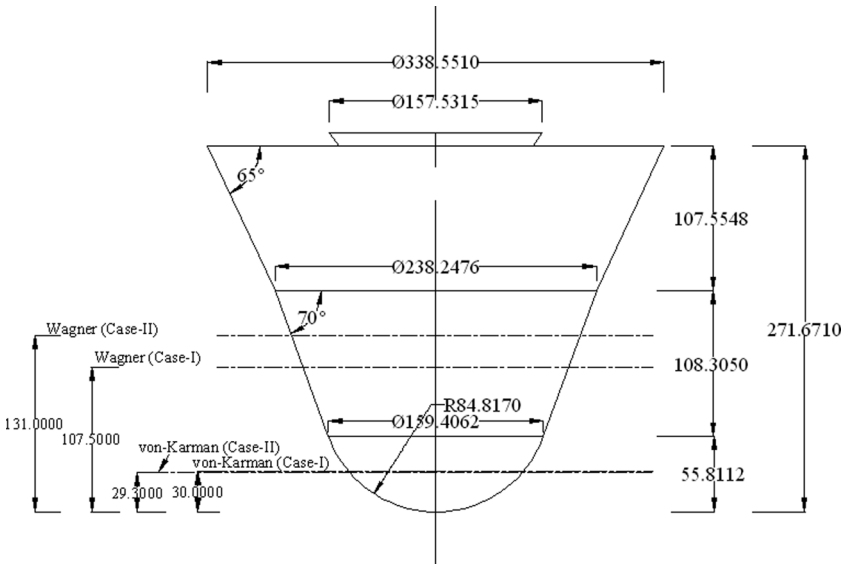

Fig. 12 Equivalent radius of the WLO model

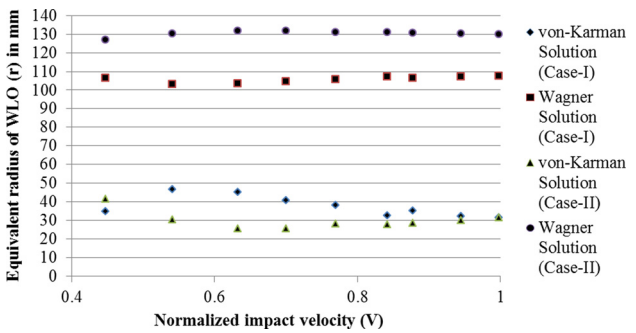

Fig. 13 Equivalent radius (*r*) of the WLO for different normalized velocities of impact for drop test I and drop test II using von Karman and Wagner approaches

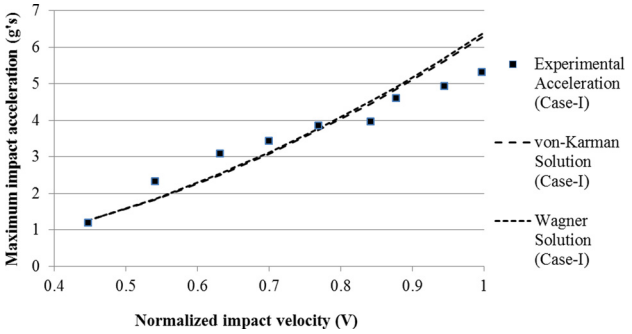

Fig. 14 Maximum impact accelerations calculated based on the mean equivalent radius (*r) of the WLO for different normalized velocities of impact for drop test I using von Karman and Wagner approaches**

obtain those values of the radii which would give the same experimental impact accelerations corresponding to the impact velocities. Observe that from Fig. 13 the values of equivalent radius (r) of the WLO model remain almost constant for different velocities of impact for both cases.

The next step is to compare the accelerations obtained experimentally (drop test I and II) to those obtained by using a mean equivalent radius (r^*). The values of r^* were obtained by taking the mean of all the equivalent radii obtained for different impact velocities corresponding to their respective impact accelerations. For each r^* obtained for each case, the impact accelerations were calculated by varying the impact velocity. Figures 14 and 15 show the comparison for the maximum impact accelerations and those obtained by the mean equivalent radius (r^*) for drop test I and II, respectively.

Figures 14 and 15 show that the maximum impact acceleration obtained by both the semianalytical models compare well with those obtained experimentally. It is interesting to note that the acceleration values obtained by von Karman and Wagner solutions produce accelerations that are similar ascertaining the importance of the shape of the WLO during water impact. (Note that we call the proposed approximate estimation procedure as "semianalytical" because experimental data is needed to determine an important parameter, namely, the equivalent radius.)

Discussion and Comparison. An important aspect is the comparison of the shape of the space capsule used for the Indian and American space missions. The WLO used for the Indian space mission is conical in shape with a rounded nose than compared to the convex shape of the base used for all the American space missions. This significantly inhibits the comparison with the literature available for ACM or other American space missions. The present work is the first of its kind in testing a scaled-down model of a WLO (with a conical shaped base) impacting ocean waters.

An attempt was made to study the impact dynamics of the WLO during and after touchdown with water surface using an underwater camera but they were discarded as the results obtained were not reliable. The hydrodynamic response of the WLO upon water impact which constitutes of measurements such as peak impact acceleration and peak impact pressure can only be used to qualitatively justify the experimental drop tests.

For the WLO weighing 2.03 kg (drop test I), the acceleration time series for a 10 m/s velocity of impact gives a peak acceleration of 52.17 m/s^2 ($\sim$5.2 g) and a touchdown pressure of 26 kPa and for the WLO tests with the electromagnetic release with an increased mass of 3.5 kg of the model (drop test II), the peak acceleration was found to be 36.5 m/s^2 ($\sim$3.6 g) and the touchdown pressure was computed as 41 kPa. In addition, for both

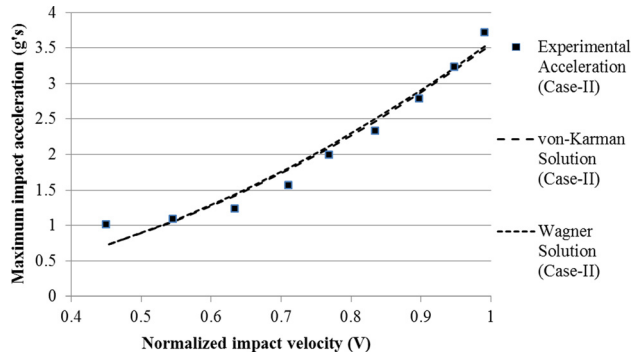

Fig. 15 Maximum impact accelerations calculated based on the mean equivalent radius (r^*) of the WLO for different normalized velocities of impact for drop test II using von Karman and Wagner approaches

independent experimental data sets, the peak force was proportional to the square of the impact velocity, which is in good agreement with Kaplan's theoretical results. Hence, a formal comparison between the two cases cannot qualitatively demonstrate the efficiency of one case over the other. Instead, for an end user, an increased weight of WLO provides a measure of the reduction of the accelerations (3.6 g in drop test II compared to 5.2 g in drop test I).

The peak impact force experienced by the model obtained using the model mass and measured acceleration is 105.9 N for drop test I compared to 127.7 N for drop test II. Comparison of drop heights to theoretical and experimental velocities depict a very good agreement for both the cases, ascertaining the accuracy of the impact accelerations measured experimentally for successive drop heights.

In order to describe the physics of the slamming problem, the maximum pressure obtained was compared to the pressure calculation when a circular cylinder slams the water surface [7]. The fluid behavior is incompressible at pressure values significantly below the acoustic pressure bound ($\rho c_e V = 14{,}500$ kPa). The measured values of maximum impact pressure for both the drop test cases were 26 and 41 kPa for drop tests 1 and 2, respectively, which are well below the pressure bound confirming the main assumption that the fluid is incompressible [5].

The WLO was assumed as rigid for the convenience of comparing experimental results with closed form solutions for maximum accelerations predicted by the classical von Karman and Wagner. The maximum radius of the base of the model is 338.5 mm, whereas the radius of the conical portion impacting the water surface is 84.8 mm, which is primarily responsible for the large difference between experimental and analytical estimates. An improved approximate solution procedure using an "equivalent" radius concept integrating experimental results with the von Karman and Wagner closed-form solutions is proposed and developed in detail.

Concluding Remarks

An important aspect in the assessment of recovery and escape systems of water-impact rigid bodies is the performance of these bodies in ocean water landing. The primary objective of this study is to examine the dynamic response of a conical shaped rigid body with a spherical nose (WLO) during water impact by conducting experiments using a 1/6th Froude-scale model and two independent drop mechanisms. Drop test I involved dropping the rigid body using a rope and pulley arrangement, while drop test II employed an electromagnetic release to drop the rigid body. The effects of varying the vertical velocity and the rigid body weight are identified and the trend obtained helps the readers to comprehend the conditions that must be avoided during a water impact. The hydrodynamic parameters such as peak acceleration and touchdown pressure were measured and the dynamic response of the rigid body during touchdown was observed. The peak values of acceleration for drop tests I and II are 5.2 g and 3.6 g, respectively. If a crew member onboard the rigid body (WLO) cannot withstand impact accelerations over 5 g, these results will give a glimpse of the initial conditions which will keep the peak impact accelerations under the specified limits. Note that the maximum impact accelerations obtained in the experiments will directly predict the prototype values according to Froude scaling (scale factor = 1). Therefore, the maximum impact acceleration for a prototype is expected to be approximately 5 g.

An important aspect is the accuracy and reliability of the experimental results in predicting the impact accelerations and touchdown pressures obtained from both the experimental cases. Results from both the experimental data sets show that the impact acceleration and touchdown pressure increases practically linearly with the increase in the height of the drop.

The reliability of the experimentally measured maximum accelerations was calibrated with classical von Karman and Wagner approximate closed-form solutions. For a conical bottomed rigid body, the analytical results show that there is a large difference between the experimental peak impact accelerations and those obtained by these analytical estimates. The large difference can be partly attributed to the unique shape of the rigid body considered (i.e., the WLO) and partly due to the assumptions of the formulations for both von Karman and Wagner approaches. Owing to the large difference between the experimental accelerations and those provided by von Karman and Wagner approaches, an improved approximate solution procedure using an equivalent radius (r) of the rigid body (WLO) was estimated to understand the physics of the impact. It can be observed that the von Karman approach tends to estimate a lower value of the radius of the conical portion, whereas the Wagner approach tends to estimate a higher value of the impact radius.

As the effect of local rise up of the water is significant during water entry of a rigid 3D rigid body, the von Karman predictions for maximum impact accelerations are not significant in determining the maximum impact accelerations for the water entry of the WLO. Based on the equivalent radius approach, the approximate analytical solutions of von Karman and Wagner can be used to obtain design maximum accelerations of the WLO model consistent with experimental results. Furthermore, the mean equivalent radius (r^*) was computed to analytically estimate the maximum impact accelerations (for varying impact velocities). Results show the maximum impact accelerations obtained by both the semianalytical estimates compared reasonable well with the experimental acceleration values.

In order to achieve accelerations comparable to the closed-form solutions, the analytical results show that, for the design of a WLO, the Wagner approach provides a correct estimate of the equivalent radius of the WLO. It is, however, interesting to note that the acceleration values obtained by von Karman and Wagner solutions produce accelerations that are similar ascertaining the importance of the shape of the WLO during water impact.

Finally, several areas are worthy of mention at this juncture. Model testing is needed over a wider range of conditions to include improved tests which vary the speed, weight, and entry angle and under realistic conditions existing in the oceans. The model used for the drop tests should be specifically designed to avoid structural vibrations.

Future work can also include more in-depth analysis of the vehicle impact pressures, fully deformable vehicles, and floatation studies. Numerical simulations of the rigid body splashdown can be performed and the possibility of combining the finite element package with a computational fluid dynamics package could more accurately simulate the hydrodynamics during impact.

Acknowledgment

Financial support from the US Office of Naval Research Grants N0014-11-1-0094 and ONR-N00014-13-1-0849, and the Department of Energy Grant DE-FG36-08GO18179-M001 for the first and second author are gratefully acknowledged.

References

[1] Von Karman, T., 1929, "The Impact of Seaplane Floats During Landing," NACA TN 321, National Advisory Committee for Aeronautics, Washington, DC.
[2] Baker, E., and Westine, S., 1967, "Model Tests for Structural Response of Apollo Command Module to Water Impact," J. Spacecraft Rockets, **4**(2), pp. 201–208.
[3] Kaplan, A., 1968, "Simplified Dynamic Analysis of Apollo Water Impact, Including Effects of the Flexible Heat Shield," 11176-11176-6004-R0-00, TRW, Redondo Beach, CA.
[4] Miloh, T., 1991, "On the Initial-Stage Slamming of a Rigid Sphere in a Vertical Water Entry," Appl. Ocean Res., **13**(1), pp. 43–48.
[5] Brooks, J. R., and Anderson, L. A., 1994, "Dynamics of a Space Module Impacting Water," J. Spacecraft Rockets, **31**(3), pp. 509–515.
[6] Zhao, R., Faltinsen, O. M., and Aarsnes, J. V., 1996, "Water Entry of Arbitrary Two-Dimensional Sections With and Without Flow Separation," *Proceedings of the 21st Symposium on Naval Hydrodynamics*, National Academy Press, Washington, DC, pp. 408–423.
[7] Faltinsen, O. M., 1990, *Sea Loads on Ships and Offshore Structures*, Cambridge University Press, Cambridge, UK.
[8] Faltinsen, O. M., 1997, "The Effect of Hydroelasticity on Slamming," Philos. Trans. R. Soc. London Sect. A, **355**, pp. 575–591.
[9] Faltinsen, O. M., 1999, "Water Entry of a Wedge by Hydroelastic Orthotropic Plate Theory," J. Ship Res., **43**(3), pp. 180–193.
[10] Scolan, Y. M., and Korobkin, A. A., 2001, "Three-Dimensional Theory of Water Impact. Part 1. Inverse Wagner Problem," J. Fluid Mech., **440**, pp. 293–326.
[11] Korobkin, A. A., 2005, "Three-Dimensional Nonlinear Theory of Water Impact," Proc. 18th International Congress of Mechanical Engineering (COBEM), Ouro Preto, Minas Gerais, Brazil.
[12] Korobkin, A. A., and Scolan, Y. M., 2006, "Three-Dimensional Theory of Water Impact. Part 2. Linearized Wagner Problem," J. Fluid Mech., **549**, pp. 343–373.
[13] Seddon, C. M., and Moatamedi, M., 2006, "Review of Water Entry With Applications to Aerospace Structures," Int. J. Impact Eng., **32**, pp. 1045–1067.
[14] Scolan, Y. M., and Korobkin, A. A., 2012, "Hydrodynamic Impact (Wagner) Problem and Galin's Theorem," Proc. 27th International Workshop on Water Waves and Floating Bodies, Copenhagen, Denmark.
[15] Faltinsen, O. M., 2005, *Hydrodynamics of High-Speed Marine Vehicles*, Cambridge University Press, Cambridge, UK.
[16] Wagner, H., 1932, "Transformation Phenomena Associated With Impacts and Sliding on Liquid Surfaces," Math. Mech., **12**(4), pp. 193–215.
[17] Wang, J. T., and Lyle, K. H., 2007, "Simulating Space Capsule Water Landing With Explicit Finite Element Method," 48th AIAA/ASME Conference, April, Waikiki, HI, pp. 23–26.
[18] Hirano, Y., and Miura, K., 1970, "Water Impact Accelerations of Axially Symmetric Bodies," J. Spacecraft Rockets, **7**(6), pp. 762–764.